



Spatial correlations in permeability distributions due to extreme dynamics restructuring of unconsolidated sandstone

Alex Hansen^{a,*}, Liacir S. Lucena^b, Luciano R. da Silva^b

^a Department of Physics, Norwegian University of Science and Technology, N-7491 Trondheim, Norway

^b Universidade Federal do Rio Grande do Norte, UFRN, Departamento de Física C. P. 1641, Natal-RN, 59072-970, Brazil

ARTICLE INFO

Article history:

Received 6 April 2010

Received in revised form 13 August 2010

Available online 20 October 2010

Keywords:

Permeability

Self-organized criticality

Transport in porous media

ABSTRACT

We propose a model for porous sandstone formation from unconsolidated sand based on a series of restructuring events where the local pressure difference due to flow in the sand is the largest. We investigate the local and global permeability distributions after steady state has been reached. Whereas we find no spatial correlations in the local permeability distribution, the distribution of inverse permeability shows spatial correlations consistent with a fractional Brownian noise characterized by a Hurst exponent of 0.88(9). The global permeability of the system shows time fluctuations as restructuring proceeds consistent with self-affinity characterized by a Hurst exponent of 0.25(3), crossing over to white noise at larger time scales.

© 2010 Elsevier B.V. All rights reserved.

1. Introduction

The understanding of flow in porous media plays an essential role in essential industries such as the exploitation of oil reservoirs. An important input in the reservoir simulators used by the industry is the permeability distribution of the grid blocks one defines. This spatially correlated distribution is often constructed using geostatistics. A particularly promising approach is that of *fractal geostatistics* [1], using the methods of artificially generating permeability landscapes that are statistically indistinguishable from those observed in core samples [2,3].

First proposed by Hewitt [4], it is now widely believed that the spatial correlations seen in porosity well logs are consistent with the signal being a *fractional noise*. That is, if $\phi(x_i)$ is the porosity at position x_i along the well, measured at intervals Δx , and

$$\tilde{\phi}(f_k) = \Delta x \sum_{j=0}^{N-1} \phi(x_j) e^{if_j \Delta x} \quad (1)$$

is the Fourier transform at discrete frequencies $f_k = (k-1)\Delta f$ where $\Delta f = 2\pi/N\Delta x$, then the Fourier spectral density scales as

$$S(f_k) = |\tilde{\phi}(f_k)|^2 \propto \frac{1}{f_k^{2H-1}}, \quad (2)$$

where $0 < H < 1$ is the *Hurst exponent* of the fractional noise.¹

* Corresponding author. Tel.: +47 73593649; fax: +47 73597710.

E-mail addresses: Alex.Hansen@ntnu.no (A. Hansen), liacir@dfe.ufrn.br (L.S. Lucena), luciano@dfe.ufrn.br (L.R. da Silva).

¹ The “derivative” of a self-affine function is a fractional noise. If the self-affine function is characterized by a Hurst exponent H , where $0 < H < 1$, the fractional noise is characterized by a Hurst exponent $H - 1$. It is common to add one to the Hurst exponent of the fractional noise in order to bring it into interval $[0, 1]$. However, it is then necessary to specify that the stochastic function is a noise.

Even though porosity is only one out of many variables that determine the permeability of porous rocks, several heuristic relations between these two quantities have been proposed [1,5]. A standard correlation common in the literature is

$$k = a10^{b\phi}, \quad (3)$$

where a and b are constants. Another much-used correlation is the Kozeny–Carman formula [6–8]

$$k = C \frac{\phi^3}{(1 - \phi)^2}, \quad (4)$$

where C is a constant.

As long as the permeability k is a one-to-one function of the porosity ϕ , the permeability field will show the same scaling properties of the spatial correlations as the porosity field. This is the case both for Eq. (3) and the Kozeny–Carman correlation in the physical range $\phi \in [0, 1]$ —and should be a feature of all permeability–porosity correlations.

It is the aim of this paper to propose a mechanism by which the observed spatial correlations may have been generated. We describe the mechanism through the introduction of a model. The model is a generalization of the Bak–Sneppen model, which has become the quintessential example of self-organized criticality [9].

We test out the model in two dimensions, whereas natural sandstone is three-dimensional. We do therefore not expect that the results we present in the following will be quantitatively correct. On the other hand, the flow properties of unconsolidated granular materials in two dimensions have been investigated experimentally; see e.g. Ref. [10] and the references therein. In such two-dimensional systems the present results should be directly applicable.

Our main result is that the ensuing permeability distribution shows white noise-type spatial correlations that even though the ensuing permeability distribution shows white noise-type spatial correlations, the distribution of the *inverse* permeability has the character of a fractional Brownian noise characterized by a Hurst exponent equal to 0.88. Through the monotonic relation between permeability and porosity, the same properties will hold for the correlations in the porosity distribution.

It is surprising, but no contradiction in the different correlations of the permeability and its inverse. We see e.g. a difference in character between a stochastic function and its inverse in the common random walk in one dimension, whereas the random walk itself is *self-affine* characterized by a Hurst exponent equal to 1/2, its inverse forms a *fractal* set of infinite spikes with fractal dimension 1/2 [11]. The model consists of envisioning a granular packing which is undergoing internal restructurings due to local pressure differences while being flooded. We monitor the permeability fluctuations of the entire system as a function of time, measured in terms of the number of internal restructurings. We find that these fluctuations are self-affine up to some crossover time scale. On larger scales than this, it becomes white noise. The Hurst exponent characterizing the fluctuations is 0.25. We also identify two dynamical exponents, one associated with correlating the permeabilities, and one associated with decorrelating the permeabilities, having the values 1.87 and 2.5 respectively.

In Section 2 we describe in detail the model. The following section is devoted to the results the model gives, and which were summarized above. We conclude in Section 4.

2. Model

We model the porous medium as a square lattice placed at 45° with respect to an inlet and an outlet forming two opposite edges of the lattice; see Fig. 1. The lattice has size $L \times L$ and the boundaries are periodic in the direction orthogonal to the average flow direction. Each bond ij (see Fig. 1) in the lattice is a tube with a given permeability k_{ij} , a cross section w and a length l . The fluid that flows in the network has a viscosity μ . If the pressure difference along the bond is Δp_{ij} , the flux through bond, q_{ij} , is given by the Darcy law

$$q_{ij} = \frac{k_{ij}w}{\mu l} \Delta p_{ij}. \quad (5)$$

We assume that the disorder in the model is reflected in a distribution of permeabilities k_{ij} , while all other parameters are constant. The bonds in the lattice represent the pore space between unconsolidated or weakly consolidated grains, whereas the nodes of the dual lattice represent the grains; see Fig. 1. We now assume that if the pressure difference across a bond exceeds some threshold t_{ij} , the two grains that make up the affected pore space, are perturbed. This in turn affects the six pore spaces (bonds) that constitute the other sides of the two grains. In keeping with the philosophy of minimizing the number of adjustable parameters, we assume that the thresholds are all equal. Hence, the bond with the largest pressure difference across it, is the one where the next restructuring will take place. The restructuring itself is modeled through replacing the permeability of the bond that carried the largest pressure difference and those of the neighbors defined in Fig. 1 by new, uncorrelated permeabilities drawn from the same probability distribution as that used to generate the initial permeabilities.

The model has a strong linkage to the Bak–Sneppen model, which was constructed to account for evolutionary bursts [9]. It consists of a one-dimensional chain, where each node is assigned a random number. The smallest random number is identified and this, and its two nearest neighbors are replaced by new random numbers from the same distribution as used initially. It is important to notice that without changing the neighbors, the distribution of numbers along the chain never

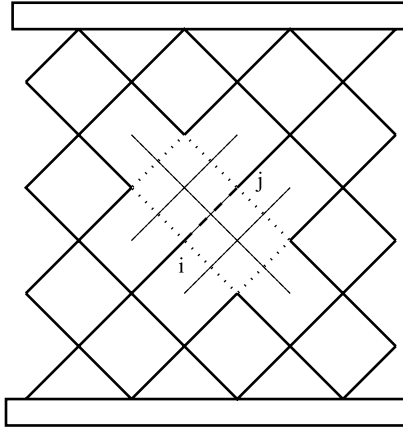


Fig. 1. Each link in the lattice shown with thick lines or dotted lines represents the space between two adjacent sand grains. The sand grains themselves are situated at the nodes of the *dual* lattice, shown with thin lines. A portion of the dual lattice is shown as dot-dashed thin bonds. The nodes of this lattice represent the grains. The bonds of the original lattice represent the pore space between the grains. Restructuring affects the two neighboring grains to the pore space that initiated it, shown as a dashed bond. This in turn affects the pore spaces (bonds) that are noted using dotted bonds.

reaches a steady state. Furthermore, no self-organized criticality is observed in this case. Variations of this model were used by Török et al. [12–14] to model shear bands in granular packings. The model described in Ref. [12] was implemented on a square lattice, each node is assigned a random number. These random numbers are interpreted as thresholds for local restructuring caused by shear. A band of restructurings spanning the lattice in the direction parallel to the average shear will form along the path such that sum of thresholds is minimum, $\min_{\mathcal{P}} \sum_{ij \in \mathcal{P}} t_{ij}$. The random numbers along this path are all replaced by new ones, and the process is repeated. It was noted that this procedure leads to a slow aging in the system [14]. This aging is closely related to the non-stationarity observed in the original Bak–Sneppen model. The present model takes a step even further way from the original Bak–Sneppen model than the shear band model in that the extreme dynamics of the model is connected to a pressure field that is found by solving the Kirchhoff equations for the network. The restructuring that takes place is not directly changing the extreme value, but rather the value of the random numbers that determine the extreme value through the solution of the Kirchhoff equations.

We solve the Kirchhoff equations using the conjugate gradient method [15]. Choosing units to that the Darcy equation becomes $q_{ij} = k_{ij} \Delta p_{ij}$, we set the pressure difference across the lattice to be equal to one, $\Delta P_1 = 1$. We then determine the pressure differences across all bonds, Δp_{ij}^1 , where the superscript refers to the unit pressure difference across the lattice. We then identify

$$\Delta P_b = \frac{1}{\max_{ij} \Delta p_{ij}^1}, \tag{6}$$

which is the pressure difference across the lattice at which the next restructuring takes place. This is precisely the idea of the Bak–Sneppen model, which may be seen as a one-dimensional version of the present model: local restructuring occurs where local pressure gradient is the largest. We then calculate the permeability of the lattice,

$$K = K \Delta P_1^2 = \sum_{ij} k_{ij} (\Delta p_{ij}^1)^2. \tag{7}$$

This in turn allows us to determine the flux entering the lattice at the point of the next restructuring,

$$Q_b = K \Delta P_b. \tag{8}$$

In order to clarify further the relation between the present model and the Bak–Sneppen model in one dimension, consider a chain of permeabilities—a one-dimensional porous medium. Each bond in the chain is allocated a permeability k_{ij} . The indices i refer to the nodes. If a flux Q is pushed through the chain, there will be a pressure difference $\Delta P = Q/K$ between the inlet and outlet of the chain, where $K = \sum_{ij} k_{ij}^1$. The pressure difference between neighboring nodes i and j is $\Delta p_{ij} = Q/k_{ij}$. If we assume that a rearrangement occurs for the bond with the largest pressure difference across it, which in one dimension is given by $\min_{ij} k_{ij}$. We then exchange the value of this permeability and its two nearest neighbors by new values. This is precisely the Bak–Sneppen model.

3. Results

The initial permeability distribution was chosen to be uniform on the interval $[0, 1/2]$. The upper limit of $1/2$ was chosen such that if all k_{ij} were set to this value, the global permeability K would be equal to 1. We show in Fig. 2 (upper figure) the

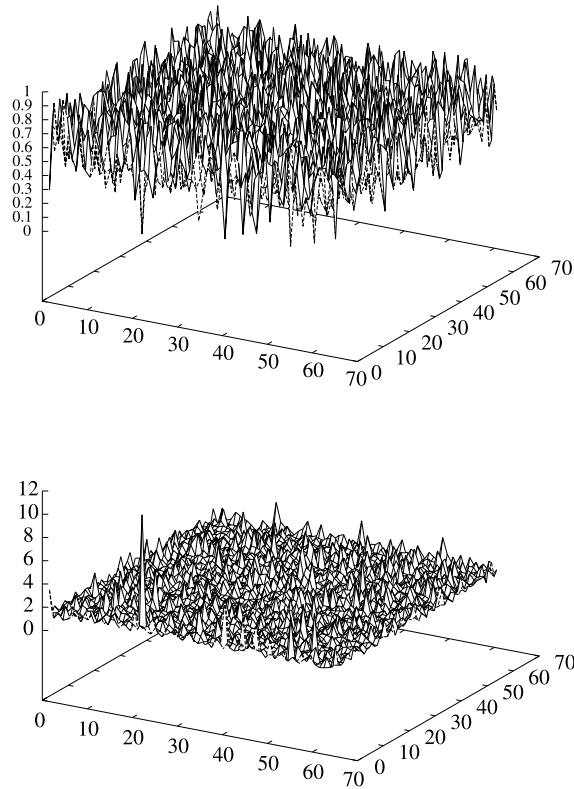


Fig. 2. Spatial distribution of local permeabilities (upper figure) and local inverse permeabilities (lower figure) on a 64×64 lattice after 1100 000 updates.

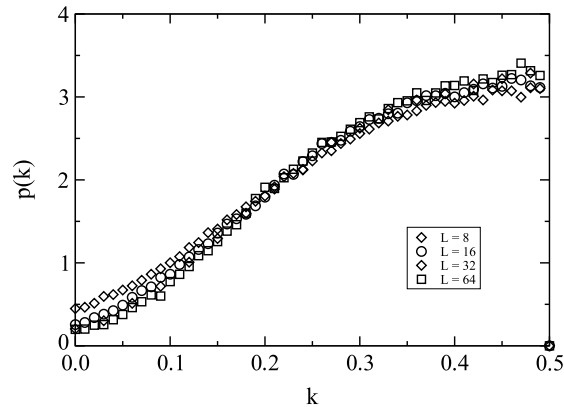


Fig. 3. Distribution of local permeabilities after 1100 000 updates.

permeability distribution of a 64×64 lattice after 1100 000 restructurings. There are no discernable spatial correlation in this distribution. Using average wavelet Coefficient method [16] to determine whether the distribution has any scaling properties reveals no such properties. Measuring $\Delta K = \sqrt{\langle K^2 \rangle - \langle K \rangle^2}$, where $\langle \dots \rangle$ signifies an average over configurations, gives $\Delta K = 0.12$ irrespective of the system size L . On the other hand, the *inverse* permeability distribution shows power-law type correlations consistent with a fractional noise characterized by a Hurst exponent $H = 0.88$ (with an accuracy of about 10%). This is shown in Fig. 4, where we have used the Average Wavelet Coefficient (AWC) Method to analyse 64×64 surfaces [16]. The average wavelet coefficients calculated along one-dimensional stripes along the surface scale as $W(a) \sim a^{0.38}$. The Hurst exponent of the trace is then $0.38 - 1/2 = -0.12$. As we find a negative value, we infer that we are dealing with a fractional *noise*. Following convention, we then add unity to the Hurst exponent to bring it into the unit interval; see Footnote 1. We show in Fig. 2 (lower figure) the inverse of the permeability distribution for the same 64×64 lattice as shown in the upper figure. The two figures (upper and lower) look qualitatively very different.

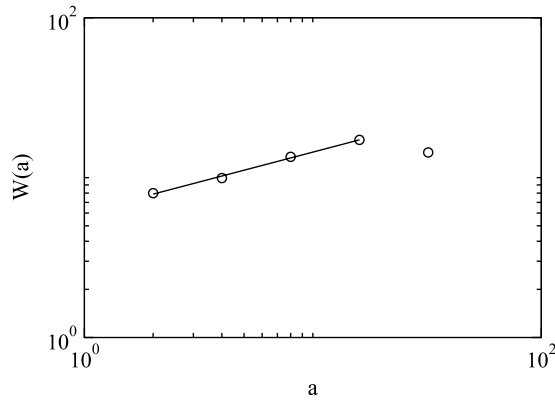


Fig. 4. Average wavelet coefficient (AWC) analysis of inverse permeability spatial distribution based on 64 samples of 64×64 lattices. The exponent of the straight line is 0.38, corresponding to the spatial distribution being a fractional noise characterized by a Hurst exponent $H = 0.88$.

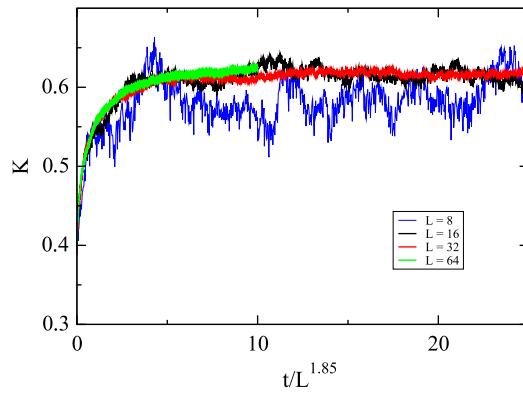


Fig. 5. Permeability as a function of elementary updates t rescaled by L^τ , where $\tau = 1.85$.

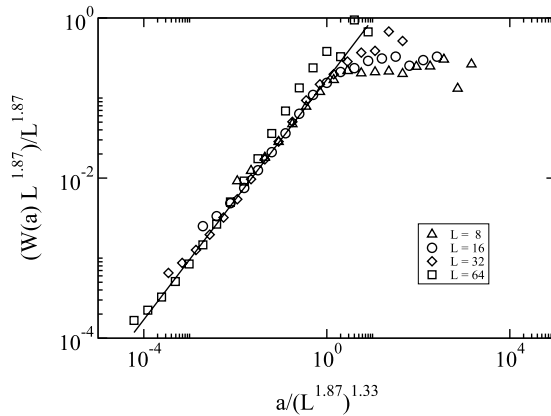


Fig. 6. AWC analysis of permeability fluctuations. The straight line corresponds to a power law with exponent 0.75. Data collapse of the part having a power law of 0.75 is achieved by scaling the wavelet coefficient $W(a)$ s by $L^{1.87}$, while full data collapse is achieved by scaling $W(a)L^{1.87}$ by $L^{-1.87}$ and the scale a by $(L^{-1.87})^{1.33}$.

Fig. 3 shows the steady-state permeability distribution. The extreme dynamics targets the large pressure differences across bonds. There occur for low-permeability bonds, and, hence, these get depleted. The distribution shows as a result a skewness towards large permeabilities. Furthermore, we note that no aging is observed in the system. This is a result of changing not only the extreme bond, but also its neighbors.

The permeability of the lattice fluctuates as the restructurings proceed [17]. Fig. 5 shows the development of the permeability as a function of time, measured in terms of the number of restructurings, t . By scaling the time variable by $L^{-1.85}$, the permeability curves collapse for different system sizes. Hence, we conclude that there is a correlation time t_c

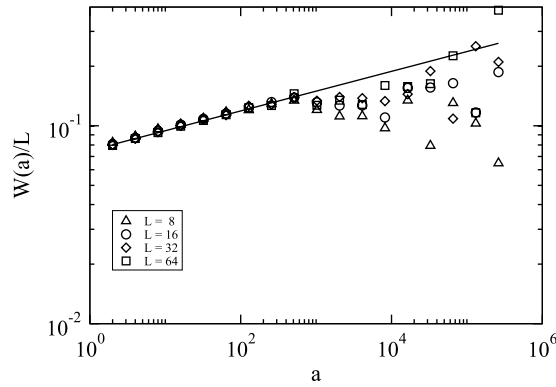


Fig. 7. AWC analysis of the pressure fluctuations. The straight line corresponds to a power law with exponent 0.1. Data collapse is achieved by scaling the wavelet coefficient $W(a)$ s by L^{-1} .

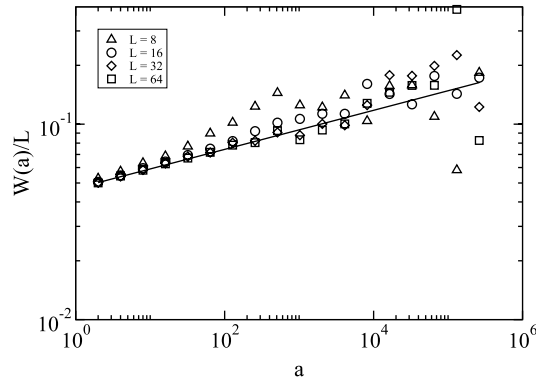


Fig. 8. AWC analysis of the flux fluctuations. The straight line corresponds to a power law with exponent 0.1. Data collapse is achieved by scaling the wavelet coefficient $W(a)$ s by L^{-1} .

connected to a length scale ξ as

$$t_c \sim \xi^{\tau_c}, \quad (9)$$

where $\tau_c = 1.85$. We show in Fig. 6 the average wavelet coefficient of the permeability $W(a)$ as a function of time scale a . The curves reveal a power law with an exponent 0.75, corresponding to a self-affine trace with Hurst exponent $H = 0.25$ (with an accuracy of about 10%). At larger time scales, there is a crossover to a flat part. This corresponds to white noise. Without rescaling either of the axes, the white-noise part of the curves fall on top of each other. Hence, the long-time fluctuations of the permeability are independent of system size. However, by rescaling the ordinate in Fig. 6 by $W(a) \rightarrow W(a)L^{1.87}$ will produce data collapse in the scaling part of the signal. The exponent 1.87 is the τ exponent defined in Eq. (9). Now, rescaling the ordinate $W(a)L^{1.87} \rightarrow [W(a)L^{1.87}]/L^{1.87}$ and the abscissa by $a \rightarrow a[L^{1.87}]^{1/0.75}$ produces full data collapse. This identifies a second dynamical exponent τ_d , controlling the decorrelation time t_d ,

$$t_d \sim \xi^{\tau_d}, \quad (10)$$

where $\tau_d = 1.87/0.75 = 2.5$.

Such a crossover to white noise must exist, since self-affine fluctuations are not stationary and as the local permeabilities are bounded in the interval $[0, 1/2]$, so must the fluctuations in the global permeability.

The pressure, P_b fluctuations, and the flux, Q_b , fluctuations, Figs. 7 and 8, also decorrelate to white noise. The decorrelation time is independent of lattice size. However, rescaling the ordinate, $W(a) \rightarrow W(a)/L$, produces data collapse. The significance of this scaling is that flux *density* and pressure *gradient* are the proper intensive variables. There is a scaling part of the curves, both for pressure and flux, corresponding to a fractional Brownian motion with Hurst exponent equal to 0.6.

Figs. 9 and 10 show histograms of the avalanches in pressure P_b and flux Q_b respectively. We measure the avalanches by recording the number of restructurings that occurs from – say – P_b drops below a certain value until it again exceeds it. These values were chosen to be close to the median value of P_b and Q_b for each lattice size L : for the pressure, we used for $L = 8$, 4.1, while for the flux 2.5, for $L = 16$, we used the values 8 and 5 respectively, for $L = 32$, 15 and 10, and for $L = 64$, 30 and 20. In contrast to the Bak–Sneppen model, the avalanches do not follow power laws. Rather, they follow an exponential, with a scale that is sensitive to where the return level is set.

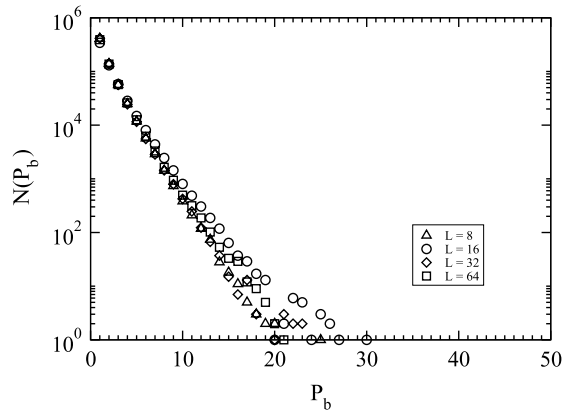


Fig. 9. Avalanche distribution N in pressure P_b for 1100 000 restructurings.

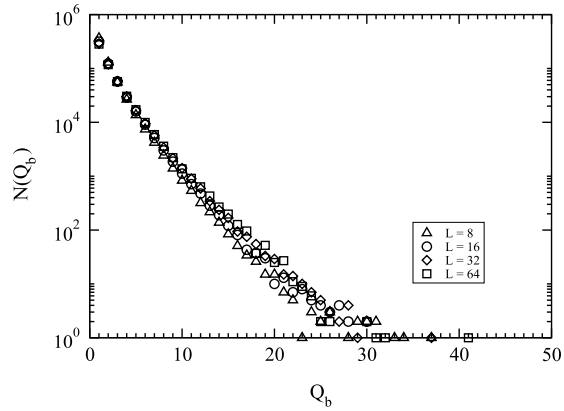


Fig. 10. Avalanche distribution N in flux Q_b for 1100 000 restructurings.

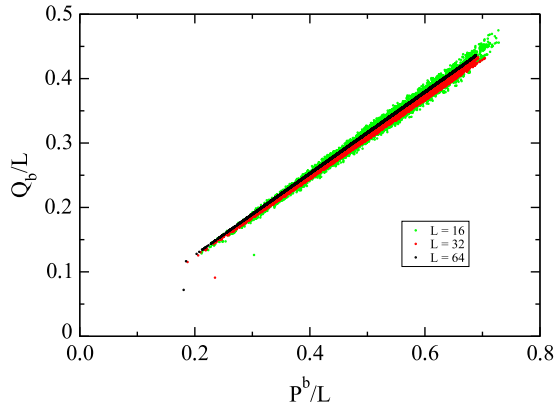


Fig. 11. Restructuring flux Q_b vs. restructuring pressure P_b for three lattice sizes based on 5000 restructurings recorded after the system has reached steady state. Q_b and P_b have both been rescaled to reflect local quantities.

Fig. 11 shows the restructuring flux Q_b plotted against the restructuring pressure P_b . Both quantities have been scaled by $1/L$, obtaining data collapse. The reason for this data collapse is as in Figs. 7 and 8 that flux density and pressure gradient are the proper intensive variables.

4. Discussion and conclusion

We have presented a model based on extreme dynamics for the restructuring of unconsolidated sandstone due to internal pressure gradients. We find that the permeability distribution that emerges is spatially uncorrelated. However, the global permeability correlations are self-affine with Hurst exponent 0.25(3) up to a decorrelation time t_d which scales with the system size as L^{τ_d} , see Eq. (10), where τ_d is 2.5. There is also a correlation time exponent $\tau_c = 1.87$; see Eq. (9).

The spatial correlations of the permeability do not show any power-law type correlations. However, the *inverse* distribution does. This is understandable from examining Fig. 3. The permeability distribution is depleted towards small values and limited by the value 1/2 towards larger values. Even though we are not able to resolve the precise form of the tail of this distribution towards small values, it is likely that it proceeds all the way to zero continuously. Hence, the inverse distribution is not bounded from above and both fractional Brownian walk or noise are possible candidates for characterizing the spatial correlations. As shown in Fig. 4, we find a fractional Brownian noise with Hurst exponent 0.88(9). It is interesting to note that in the one-dimensional Bak–Sneppen model, white noise is found for both the permeability and the inverse permeability distribution.

Acknowledgements

A.H. thanks the UFRN for friendly hospitality during his stay in Natal. We thank the CNPq and ANP/CTPETRO/Petrobrás, and the Norwegian Research Council (NFR) through the Petromax program for financial support. We furthermore thank K. Sneppen for interesting discussions on this subject.

References

- [1] H.H. Hardy, R.A. Beier, *Fractals in Reservoir Engineering*, World Scientific, Singapore, 1994.
- [2] J. Feder, *Fractals*, Plenum, New York, 1988.
- [3] D.M. Tavares, L.S. Lucena, *Phys. Rev. E* 67 (2003) 036702.
- [4] T.A. Hewitt, SPE 15386, Presented at SPE Annual Tech. Conf., New Orleans, 1988.
- [5] J.H. Doveton, *Geologic Log Analysis Using Computer Methods*, American Association of Petroleum Geologists, Tulsa, 1994.
- [6] J. Kozeny, *Sitzungsber Akad. Wiss. Wien* 136 (1927) 271.
- [7] P. Carman, *Trans. Inst. Chem. Eng.* 15 (1937) 150.
- [8] A. Costa, *Geophys. Res. Lett.* 33 (2006) L02318.
- [9] P. Bak, K. Sneppen, *Phys. Rev. Lett.* 71 (1993) 4083.
- [10] B. Sandnes, H.A. Knudsen, K.J. Måløy, E.G. Flekkøy, *Phys. Rev. Lett.* 99 (2007) 038001.
- [11] A. Hansen, T. Engøy, K.J. Måløy, *Fractals* 2 (1994) 527.
- [12] J. Török, S. Krishnamurty, J. Kertész, S. Roux, *Phys. Rev. Lett.* 84 (2000) 3851.
- [13] T. Unger, J. Török, J. Kertész, D.E. Wolf, *Phys. Rev. Lett.* 92 (2004) 214301.
- [14] J. Török, T. Unger, J. Kertész, D.E. Wolf, *Phys. Rev. E* 75 (2007) 011305.
- [15] G.G. Batrouni, A. Hansen, *J. Stat. Phys.* 52 (1988) 747.
- [16] I. Simonsen, A. Hansen, O.M. Nes, *Phys. Rev. E* 58 (1998) 2779.
- [17] D.O. Maionchi, A.F. Morais, R.N. Costa Filho, J.S. Andrade, H.J. Herrmann, *Phys. Rev. E* 77 (2008) 061402.